Smart Structures and Systems, *Vol. 29, No. 1 (2022) 167-179*
https://doi.org/10.12989/sss.2022.29.1.167

Long-term condition monitoring of cables for in-service cable-stayed bridges using matched vehicle-induced cable tension ratios

Zhen Peng [1,2], Jun Li*[1,2] and Hong Hao [2]

[1] *Guangzhou University-Curtin University Joint Research Centre for Structural Monitoring and Protection against Multi-Dynamic Hazards, School of Civil Engineering, Guangzhou University, Guangzhou 510006, China*
[2] *Centre for Infrastructural Monitoring and Protection, School of Civil and Mechanical Engineering, Curtin University, WA 6102, Australia*

(*Received April 25, 2021, Revised August 27, 2021, Accepted September 9, 2021*)

Abstract. This article develops a long-term condition assessment method for stay cables in cable stayed bridges using the monitored cable tension forces under operational condition. Based on the concept of influence surface, the matched cable tension ratio of two cables located at the same side (either in the upstream side or downstream side) is theoretically proven to be related to the condition of stay cables and independent of the positions of vehicles on the bridge. A sensor grouping scheme is designed to ensure that reliable damage detection result can be obtained even when sensor fault occurs in the neighbor of the damaged cable. Cable forces measured from an in-service cable-stayed bridge in China are used to demonstrate the accuracy and effectiveness of the proposed method. Damage detection results show that the proposed approach is sensitive to the rupture of wire damage in a specific cable and is robust to environmental effects, measurement noise, sensor fault and different traffic patterns. Using the damage sensitive feature in the proposed approach, the metrics such as accuracy, precision, recall and F1 score, which are used to evaluate the performance of damage detection, are 97.97%, 95.08%, 100% and 97.48%, respectively. These results indicate that the proposed approach can reliably detect the damage in stay cables. In addition, the proposed approach is efficient and promising with applications to the field monitoring of cables in cable-stayed bridges.

Keywords: cable damage; cable-stayed bridges; cable tension ratio; damage detection; influence surface; sensor fault

1. Introduction

The cable-stayed bridges, ranged from small span footbridges to medium and long-span highway bridges, have been widely constructed around the world for its elegant appearance, desired spanning capacity and cost-effectiveness (Martins *et al*. 2015). As the main supporting components in cable-stayed bridges, the cables transmit the dead loads and traffic loads from superstructure to the tower and the backstay cables (Li and Ou 2016). To ensure the safety, durability and serviceability of cable-stayed bridges, high redundancy of tensile strength, fatigue resistance and corrosion protection are considered at the design stage (Davalos 2000). However, the fatigue damage accumulated by the heavy traffic (especially overloaded trucks) and various extreme loadings significantly reduce the average service lifespan of cables and anchorages (Bao *et al*. 2016, Li *et al*. 2012, Chen *et al*. 2016). Therefore, it is essential to develop effective methods to evaluate the healthy condition of stay cables under the operational conditions. The cable tension force can be directly measured by the load cell, fiber Bragg grating (FBG) strain sensor or indirectly measured by vibration-based and recently developed vision-based techniques (Kangas *et al*. 2012, Feng *et al*. 2017, Kim *et al*. 2017). Therefore, it is of potential to identify the condition of cables as well as the bridge healthy condition using the in-situ cable tension measurements. However, the environmental effects, sensor noise and external load effects may degrade the performance of existing cable force measurement based damage diagnosis method (Fan *et al*. 2020b, Li *et al*. 2014).

In literature, many data based or model based methods have been developed for the structural health monitoring of cable-stay bridges. The state-of-the-art review on the modal identification, damage detection and model updating and its engineering applications have been comprehensively provided in (Li and Ou 2016, Zhang *et al*. 2020). However, research on condition assessment of cables of cable-stayed bridges with only the cable tension force measurements is very limited, partly owning to the fact that damage sensitive features (DSF) derived from cable tension forces are also sensitive to the daily and long-term temperature variations and traffic patterns (Fan *et al*. 2020a). Xu and Wu (2007) comprehensively analysed the effects of seasonal temperature difference and sunshine temperature difference on the modal parameters, i.e., natural frequencies and mode shapes of cable-stayed bridges. Results showed that the variations in dynamic characteristics induced by temperature change are more significant than that due to structural damage occurred in bridge girder or cables. For eliminating the influence of environmental temperature effect, the cointegration analysis of the nonstationary tension forces measured from two or more cables was conducted in (Fan *et al*. 2020a). Then, the stationary

*Corresponding author, Ph.D.,
E-mail: junli@curtin.edu.au

ISSN: 1738-1584 (Print), 1738-1991 (Online)

cointegrated residual series were served as a damage feature to alarm the abnormality of stay cables. In Ref. (Chen *et al*. 2016), the daily and long-term temperature variation induced cable force changes were extracted by empirical mode decomposition. The residual cable forces were statistically analysed to determine the upper and lower criteria for damage detection. More recently, the vehicle induced cable tension ratio (Li *et al*. 2018) was adopted to evaluate the cable condition. According to the concept of the influence surface, cable tension ratio of a paired cable is only related to the mechanical property of stay cable and the transverse position of traffic location on the bridge deck. The effectiveness of using cable tension ratio for condition assessment of cables is verified by the long term cable forces measured from the Third Nanjing Yangtze River Bridge. Evaluation results demonstrated that the wire rupture in a cable can be identified. However, as mentioned in Ref. (Li *et al*. 2018), the scenarios from single vehicle located on the bridge should be separated from the measured raw data to avoid the influence of multiple vehicles on the bridge. Furthermore, inaccurate cable tension ratios may be obtained when sensor fault is occurred in one of the paired sensors, which limits its feasibility to some extent and reduces the robustness of the developed method.

This paper proposes a new approach for damage detection of cables for in-service cable-stayed bridges using matched vehicle-induced cable tension ratios. The applicability of using cable tension ratios for condition assessment of stay cables in analysing the vehicle induced cable tension forces is extended, with the awareness of sensor fault and the considerations of multiple vehicles on the bridge. Instead of calculating the cable tension ratio from a paired cable located at opposite positions (upstream and downstream sides) of the bridge, the cable tension ratio of any two cables from the same side is used. Since the longitudinal anchoring point of cables on the same side is different, there is a time shift in the arrival time instants of vehicle induced cable tension peak values. Therefore, a peak match algorithm is developed to synchronize the vehicle arrival time instants. The matched cable tension ratio between a pair of cables located on the same riverside is defined as damage feature. The main advantage of the proposed approach in this study is that the developed damage indicator is applicable to scenarios with multiple vehicles on different traffic lines and cables from the same side of the cable-stayed bridges. The cable tension ratio between any two cables located on the same side can be adopted to calculate the damage indicator. Therefore, the condition assessment of stay cables can be conducted, even when sensor fault is occurred in the adjacent and opposite locations of damaged cables. Fig. 1 illustrates the procedures of the proposed approach for damage detection of cables in cable-stayed bridges under operational conditions. Several important components are presented, including data preprocessing and damage sensitive feature extraction, etc.

The remaining sections of this paper are organised as follows. Section 2 provides details on the data preprocessing. In particular, the sensor fault is detected and the data measured by faulty sensors are separated from the overall datasets. A low-pass filter is applied in the raw monitoring data to separate the vehicle induced cable force variation with dead load and environment effects. Section 3 theoretically demonstrates the feasibility of extracting the damage feature from the matched cable tension ratios of cables located on the same side. Section 4 verifies the accuracy of using the proposed approach in identifying the damage of a cable occurred in an in-service cable-stayed bridge in China. In Section 5, conclusions and some discussions for future studies are provided

2. Data preprocessing

In this study, a set of actual cable force monitoring data measured from an in-service cable-stayed bridge in China in different periods and under different traffic conditions are analysed (Bao *et al*. 2021). This cable-stayed bridge has two steel towers with a main span of 648 m, with the front view shown in Fig. 2. The deck is supported by 168 stay cables (84 pairs). As shown in Fig. 2, cable pairs are numbered from 01 to 21 on the tower side to the riverside/bank side. For the definition of these cables, the first letter ‘S’ and ‘N’ stand for cables on south tower side and north tower side, respectively. The second letter ‘A’ and ‘J’ stand for cables on the bank side and riverside, respectively. For instance, SJ17 represents the No. 17 cable pair on the riverside anchored on the south tower. In each pair, the last letters ‘S’ and ‘X’, which are not indicated in Fig. 2, stand for cables on the upstream side and downstream side, respectively, for example, SJS17 and SJX17 represent the No. 17 cables on the upstream and downstream sides at the riverside of the south tower, respectively.

In particular, the cable tension force data of cables (14 cables of SJS08 to SJS14 and SJX08 to SJX14) for 10 days (2006-05-13 to 2006-05-19, 2007-12-14, 2009-05-05, and 2011-11-01) with a sampling frequency of 2Hz are obtained from the long term monitoring system to demonstrate the effectiveness and accuracy of using the proposed approach for detecting the damage in stay cables. For simplification, the above mentioned 10 selected days are referred to as day 1, day 2 to day 10 unless otherwise specified. For illustration purpose, Fig. 3 presents the actual cable force monitoring data of cable pairs from SJ08 to Cable SJ13 in these selected ten days.

Fig. 1 pipeline of proposed stay cable damage detection method

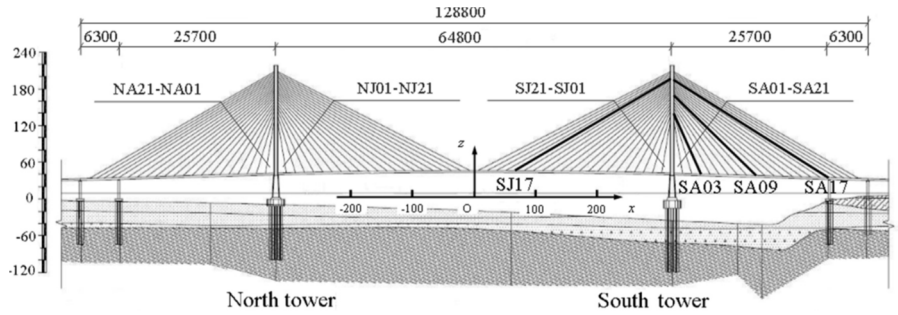

Fig. 2 Elevation of the bridge and cable numbering (Units: cm, except height in meter).

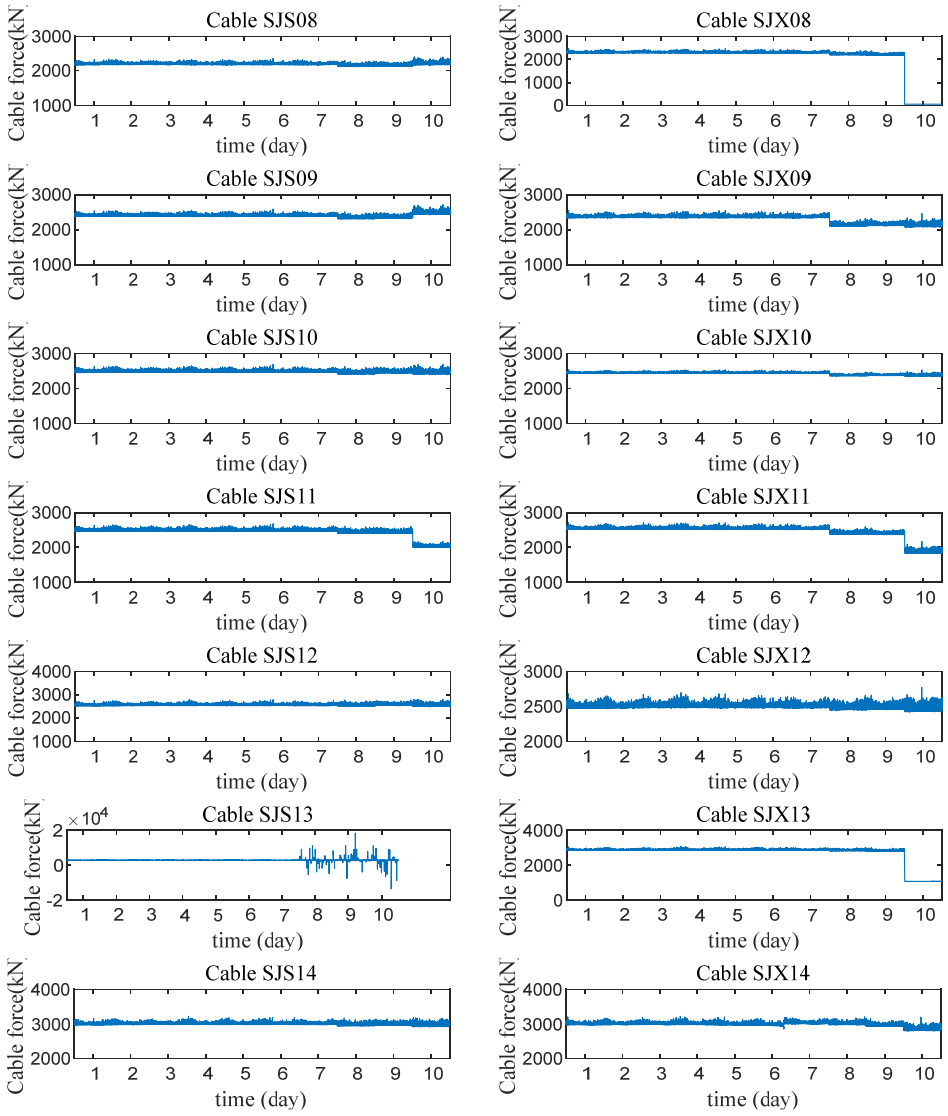

Fig. 3 The cable force of cable pair SJ08 to SJ13 in ten selected days

2.1 Numerical simulation procedure

In bridge health monitoring applications, a dense array of sensors are deployed to monitor and ensure the safety and performance of bridge during the entire life-cycle. The life expectancy of sensors are significantly shorter than that of the structure being monitored. The inevitable existence of faulty sensors may cause bias, gain, drifting, precision degradation or complete failure to the measured data (Kullaa 2013, Fan *et al*. 2019). The faulty sensors should be detected and isolated from the sensor network to ensure the accuracy and reliability of structural condition assessment. Typically, there are several categories of sensor faults. The bias, gain and drifting induced by sensor fault can be effectively eliminated by signal processing techniques like detrending and filtering. However, the data recorded by

sensors with precision degradation or complete failure should be detected and removed from the sensor network. Otherwise, the accuracy of damage detection will be significantly affected, which may even provide false identification results with monitoring data from faulty sensors.

As can be found in Fig. 3, abnormal cable force variations are observed in cables SJX08, SJS13 and SJX13, with significant drops in cable forces or large fluctuations in the measurements. In particular, obvious outliers appeared in the cable forces of cable SJS13 in the last three days. The amplitudes of these outliers are significantly higher than that of the previous seven days as well as other cables. It can be concluded that the sensor fault, i.e., the precision degradation, occurred in sensor SJS13. In addition, the measured tension forces in cables SJX08 and SJX13 significantly decrease with less oscillations in the last day. For cable-stayed bridges, the load distributed to a cable with damage (e.g., rupture of wires) will be decreased and the rest of wires inside the cable will continue to function until the full failure (Nghia and Samec 2016). In other words, the dead load, environment effects and changes in vehicle load induced cable force can be detected even when a part of wires in the cable are ruptured. Therefore, the sensor fault such as the precision degradation and complete failure of cable can generally be characterised by comparing the statistical distribution of cable forces. The histograms of cable forces in cables SJX08 and SJX13 in day 9 and day 10 are shown in Fig. 4. Under operational conditions, for the loads applied to the cable-stayed bridge including the dead load, vehicle load and other environmental effects, each source of loads has its own distribution. Therefore, it is reasonable and essential to use the Gaussian Mixture Model (GMM) to characterise the distribution of cable forces. The statistical distribution of cable forces in SJX08 and SJX13 can be well fitted by GMM with root mean squared errors (RMSE) of 0.17% and 0.29%, respectively, as shown in Figs. 4(a) and (c). For comparison, the probability density functions (PDF) of cable forces in SJX08 and SJX13 are also fitted by the generalized extreme value distribution (GEVD). However, the RMSE values obtained from GEVD are significantly higher than those from GMM. The measured cable forces of these two cables in day 9 are mainly distributed within ranges from 2175 kN to 2275 kN and from 2775 kN to 2900 kN, respectively. From the comparison with the distributions in day 10, both of the probability distribution functions and the cable force variation ranges of these two cables are significantly changed in day 10, as shown in Figs. 4(b) and (d). The cable forces of cables SJX08 and SJX13 in day 10 are best fitted by normal distribution. The mean values of cable forces in these two cables are significantly reduced to a low level, and variation range of daily cable forces is within 1 kN, which is unreasonable compared to the statistics in day 9. Therefore, it can be concluded that the complete failure occurred in sensors attached on cables SJX08 and SJX13, during the last day of measurement. To obtain accurate and reliable cable damage detection results, the measurement data of cable SJS13 from day 8 to day 10, cables SJX08 and SJX 13 in day 10 with the sensor fault are not included in the following analysis.

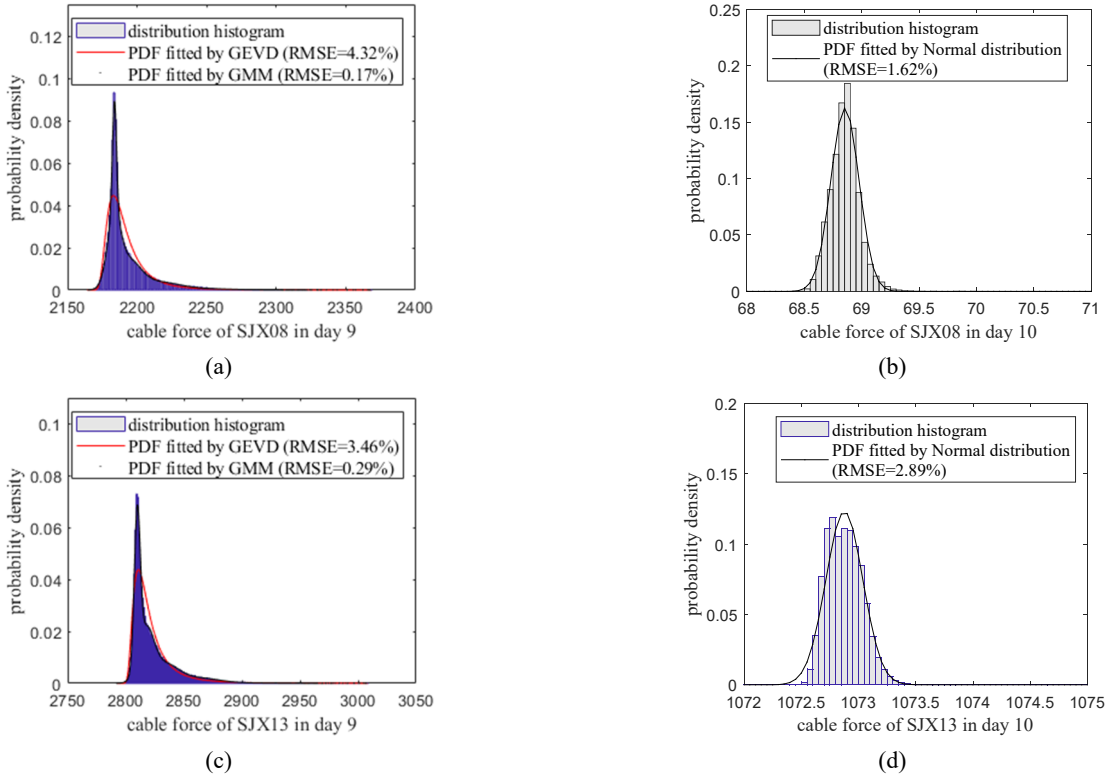

Fig. 4 Histogram of daily cable forces: (a) cable force of SJX08 in day 9; (b) cable force of SJX08 in day 10; (c) cable force of SJX13 in day 9 and (d) cable force of SJX13 in day 10.

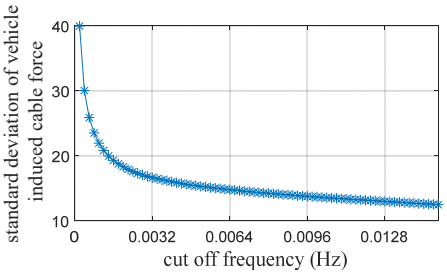

Fig. 5 Standard deviations of vehicle induced cable forces of SJS08 using different cutoff frequencies

2.2 Numerical simulation procedure

Therefore, it can be concluded that the complete failure occurred in sensors attached on cables SJX08 and SJX13, during the last day of measurement. To obtain accurate and reliable cable damage detection results, the measurement data of cable SJS13 from day 8 to day 10, cables SJX08 and SJX 13 in day 10 with the sensor fault are not included in the following analysis. The monitoring data of cable forces contain various components, including measurement noise, thermal effects, live load induced effects and dead load

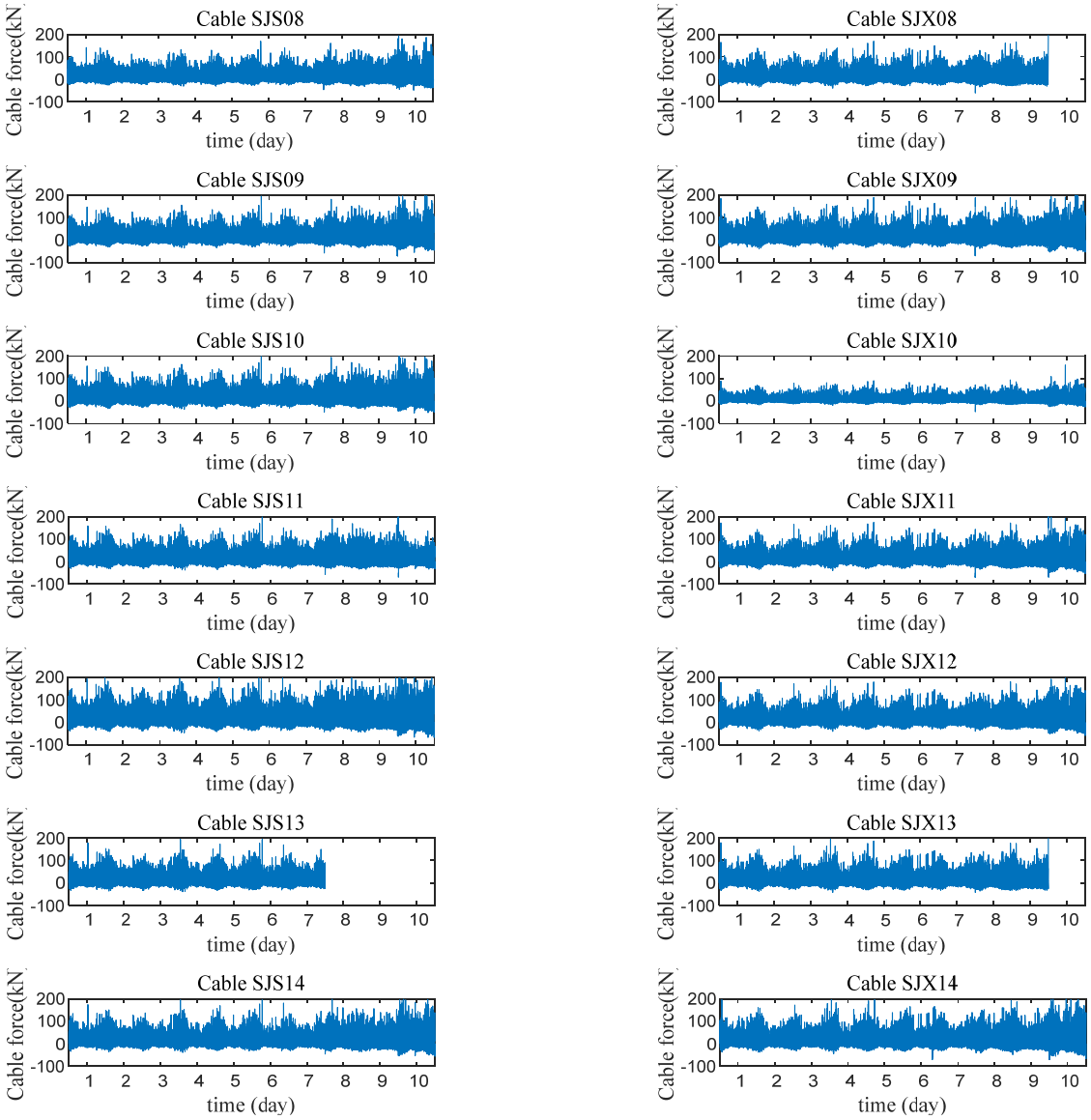

(a)

(b)

Fig. 6 (a) the vehicle induced cable forces of cable pair SJ08 to SJ13 in ten selected days; (b) zoom in view of cable SJS09 between 140~340 seconds and 1420~1620 seconds of the first day.

induced effects. The dead load induced cable tension can be viewed as a constant. Typically, the variation trend of temperature induced cable force change is much slower than that caused by the vehicle-induced loading effect. Based on this characteristic, it is possible to separate the cable tension induced by vehicle load from that from dead load and temperature effects by using the low-pass filter, signal decomposition or smoothing procedure. In this study, a low-pass filter with a cutoff frequency of 0.0032 Hz is applied to process the original data to filter out the temperature and dead load induced cable force. There is a tradeoff in the selection of cutoff frequency. The higher the cutoff frequency is selected, more information on traffic induced cable tension force will be removed. However, information in the data related to the dead load and temperature effects cannot be well removed if a relative low cutoff frequency is applied. To this end, the standard deviations of vehicle induced cable force of SJS08 with a cut off frequency ranged from 0.0002 Hz to 0.015 Hz are presented in Fig. 5. It is observed that the standard deviation values decline sharply and converge gradually with the increasing cutoff frequency. The significant decrease of standard deviation at the early stage indicates the removement of environmental effects. As shown, further increasing the cutoff frequency from 0.0032 Hz leads to insignificant reduction of the environmental and traffic effects in the data, but is expected to remove more valuable information associated to the cable force. Therefore 0.0032 Hz is selected in this study. It should be noted that the selection of an optimal cutoff frequency for the analysis varies from case to case. The vehicle induced cable tension variation of each cable are presented in Fig. 6.

3. Damage sensitive feature extraction

3.1 Existing methods based on cable tension ratios

For cable-stayed bridges, the loads from the superstructure are transmitted to the main tower and the base through the cables connected to the deck. Under operational conditions, the measured tensile force of a specific cable is related to the self-weight, vehicle load, bridge-vehicle interaction as well as environmental effect, such as temperature. The dead load transmitted to cables can be viewed as a constant value, while the traffic and temperature induced tension force is time-varying. It has been shown in existing studies (Stromquist-LeVoir *et al.* 2018). that the tensile force variation in cables is dominated by the traffic loading. For medium- and large-span cable-stayed bridges, the bridge-vehicle interaction effects and measurement noise could be ignored (Guo and Xu 2001). In literature, the cable force measurements have been used for bridge condition assessment and the moving vehicle load identification. For example, the vehicle induced cable tension ratio between the upstream and downstream cable pair is used as damage feature to detect the rupture of wires (Bao *et al.* 2021, Li *et al.* 2018). In Ref. (Bao *et al.* 2021), the vehicle load is simplified as a concentrated moving load, and the sparse regularization approach is adopted to identify the spatial location and weight of moving vehicles on the bridge. Based on the concept of the influence surface, the change in traffic induced cable tension force when multiple vehicles pass through the bridge can be expressed as

$$T_v(p) = \sum_{j=1}^{N} \sum_{k=1}^{n_j} \emptyset_{daf}\, \eta_p(x_j^k, y_j^k) P_j^k \tag{1}$$

where $T_v(p)$ represents the vehicle induced tension force transmitted to the p-th cable, $\emptyset_{daf}$ denotes the dynamic amplification factor owning to bridge-vehicle interaction effect, η_p is the influence surface (also referred to as cable tension distribution coefficient) of the p-th cable when a unit load is applied at the longitudinal position x and transverse position y. P_j^k represents the axis load corresponding to k-th axis of j-th vehicle applied on the bridge. N and n_j denote the overall number of vehicles on bridge and the number of axles of the j-th vehicle, respectively. As mentioned above, the bridge-vehicle interaction effect is not considered in this study.

It is noteworthy that $\eta_p(x,y)$ is related to the mechanical properties of the bridge structure and can be viewed as a bivariate function of concentrated vehicle load position (x,y). The influence surface of each cable is different, since the location and angle of each cable anchored to the bridge deck is different. In field practices, the influence surface of cable tension force can be determined by applying a unit force at different locations of bridge deck. In literature, the change in influence line and influence surface has been utilized as a damage sensitive feature to identify the location and extent of structural damage (Liu *et al.* 2020, Alamdari *et al.* 2019, Chen *et al.* 2015). Under the linear-elastic assumption, the influence surface $\eta_p(x,y)$ can be simplified by the product of

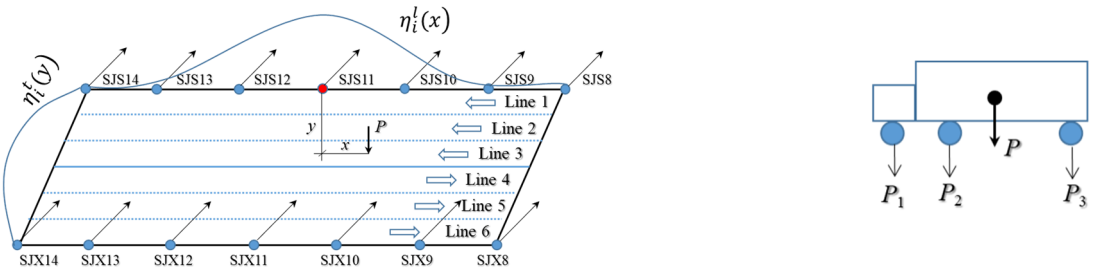

(a) (b)

Fig. 7 Illustration of a three-axis vehicle on a bridge with six lanes in both directions

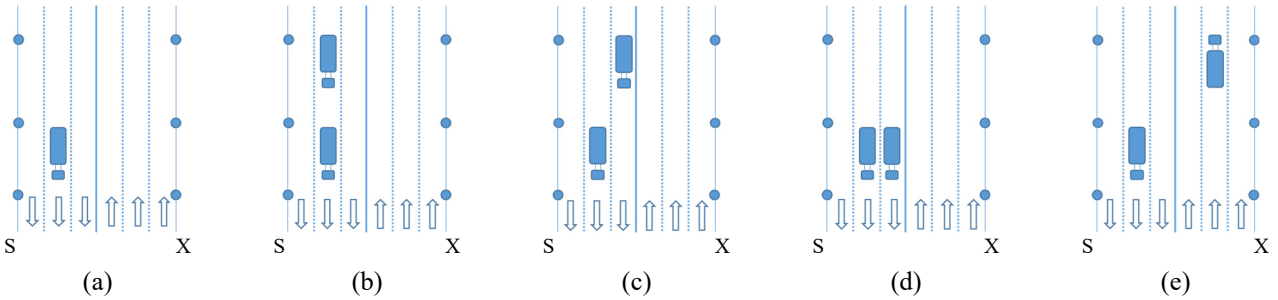

Fig. 8 Representative traffic patterns: (a) Case 1: single vehicle; (b) Case 2: multiple vehicles in the same traffic lane; (c) Case 3: multiple vehicles in different traffic lanes - same direction; (d) Case 4: multiple vehicles in different traffic lanes - same direction; and (e) Case 5: multiple vehicles in different traffic lanes – different longitudinal positions
Note: Letters 'S' and 'X' stand for cables on the upstream side and downstream side, respectively

longitudinal influence line and transverse influence line, namely

$$T_v(p) = \sum_{j=1}^{N} \sum_{k=1}^{n_j} \eta_p^l(x) \eta_p^t(y) P_j^k \tag{2}$$

where $\eta_p^l(x)$ and $\eta_p^t(y)$ represent the longitudinal and transverse cable tension influence coefficients of the p-th cable, respectively. Fig. 7 gives an illustrative example of a three-axis vehicle on a bridge with six lanes totally from both directions. For the scenario with a single vehicle on the bridge, the traffic induced cable force reaches a peak value when the vehicle crosses over the cross section where the cable is located. For any two cables located at the same side of a bridge, i.e., SJS12 and SJS13, the transverse cable tension influence coefficient will not change. For an opposite paired cable, namely one cable on the upstream side and another one on the downstream side, the longitudinal position of vehicle will be the same without considering the lane change. As a result, the cable tension force ratio between paired cables will be a constant regardless of the vehicle load, and is only related to the specific lane that the single vehicle is crossing over (Li *et al*. 2018).

Fig. 8 shows 5 representative traffic patterns, including a single vehicle on the bridge as well as multiple vehicles at different longitudinal positions and moving in opposite directions. The cable tension ratio defined in Ref. (Li *et al*. 2018) is appropriate for Case 1 and Case 2. For these two cases, the cable tension ratio can be statistically fitted by using GMM distribution with a cluster number larger than the number of traffic lanes. For multiple vehicles located at different traffic lanes (Cases 3-5), the vehicle load transmitted to each cable can be calculated by Eq. (2). Under this situation, the cable tension ratio of opposite paired cables is not only related to the traffic lane, but also to the specific weight of each vehicle. For multiple vehicle traffic Cases 3-5, using the GMM model to fit the cable tension ratio of each paired cable at opposition locations consists of uncertainties as it is traffic condition dependent. Therefore, the cable force curve corresponding to multiple vehicles in different lines (Cases 3-5) should be identified and removed. However, the cable tension force curves of Case 1 and Case 4 are similar, which make it difficult to distinguish these two cases using the existing peak detection algorithm (Vivó-Truyols *et al*. 2005). Moreover, the cable tension ratios defined in Ref. (Li *et al*. 2018) might become invalid when the sensor fault occurs in the cable that is opposite to the damaged cable, which limits its applicability in long term health monitoring. Different from the existing work, this study attempts to use the cable tension ratio between two cables located on the same side (matched cable tension ratio) as a damage feature. The transverse locations of the vehicles on the bridge for any two cables located on the same side are the same. The relative transverse position of vehicles with respect to any two cables located on the same side of bridge is the same. Therefore, the transverse location of vehicles no longer affects the vehicle-induced matched cable tension ratio. As a result, Case 3 and Case 4 are similar as Case 2 and Case 1 in Fig. 8, respectively. For Case 5, the relative distance between two vehicles in the longitudinal direction is changing, since these two vehicles in Case 5 travel to the opposite direction. There is an estimation error in the matched cable tension ratio in Case 5, owning to the changing distance between two vehicles travelling to different directions in two traffic lanes. Taking cables SJX10 and SJX11 as an example, the matched cable tension ratio between cables SJX10 and SJX11 will be larger than the actual value when the meeting point of two vehicles in Case 5 is close to cable SJX10. However, this estimation error caused by the traffic patterns in Case 5 is alleviated by using the slope of peak values collected during a period of time (1 hour data is considered in this study). The above explanations are supported by the stable and accurate damage identification results presented in Figs. 14-15 and Table 1. This study extends the feasibility of using cable tension ratios for performing damage detection of cables in cable-stayed bridges under more general traffic patterns.

2.1 The proposed approach based on matched vehicle-induced cable tension ratios

Motivated by the issues mentioned above, this study extends the feasibility of using cable tension ratios for performing damage detection of cables in cable-stayed bridges under more general traffic patterns, considering the sensor fault and operational conditions. Different from previous studies, the vehicle induced cable tension ratios of two specific cables located on the same side of bridge are

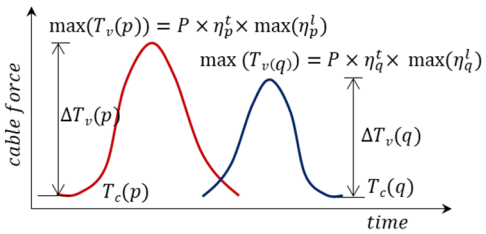

Fig. 9 Schematic diagram of the process of estimating the matched cable tension ratio

analysed. As an illustrative example, Figs. 10(a) and 11(a) present a zoom in view of vehicle induced cable tension forces in cables SJS08-SJS14 located on the upstream side at a randomly selected time duration. It can be observed from Fig. 10(a) that each cable reaches its peak tension force in a sequence from SJS14 to SJS08 with a time delay. The sequences of peak values appeared in Figs. 10(a) and 11(a) are inverted, which means that the vehicles driving through the bridge in these two representative time periods are in the opposite direction. The specific value and corresponding location of each peak are searched by using the built-in function "findpeaks" in Matlab. Therefore, the time lag effect existed in different cables subjected to the same vehicle load can be eliminated. Figs. 10(b) and 11(b) show the matched results of cable tension forces corresponding to those presented in Figs. 10(a) and 11(a), respectively, after conducting the peak matching. The matched cable tension ratio between any two cables located on the same side can be calculated as

$$\varsigma(p,q) = \frac{T_v(p)}{T_v(q)} = \frac{\sum_{j=1}^{N}\sum_{k=1}^{n_j}\eta_p^l(x)\eta_p^t(y)P_j^k}{\sum_{j=1}^{N}\sum_{k=1}^{n_j}\eta_q^l(x)\eta_q^t(y)P_j^k} \tag{3}$$

where p and q denote the p-th and q-th cables, respectively. It should be noted that the effect of spatial location and weight of vehicles on the bridge deck is always the same for each cable after the peak matching procedure. As a result, the matched cable tension force ratio $\varsigma(p,q)$ for any two cables on the same side can be viewed as an influence surface related constant value regardless of the longitudinal and transverse locations as well as the specific weight of vehicle. The main advantage of this study is that matched cable tension ratio defined in Eq. (3) is robust to different traffic patterns detailed in Fig. 8, and sensor fault can be tolerated by using different sensor pairs on the same side of the cable-stayed bridge. In existing methods for practical applications, both of the peak value and valley value of the vehicle induced cable forces should be correctly acquired to calculate the cable tension ratio defined in Eq. (3). However, as shown in Figs. 10 and 11, a certain level of oscillation is observed when the cable force reaches the valley which may be induced by the bridge free vibration when the vehicle moves out of the bridge. This cable force oscillation poses a challenge to accurately identify the valley value of vehicle induced cable force variation. An alternative way to accurately calculate the matched cable tension ratio is to estimate the slope of cable tension force

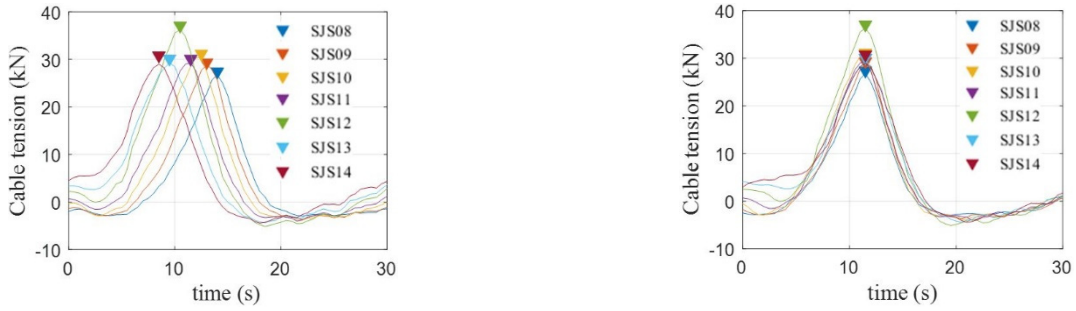

(a) (b)

Fig. 10 The cable tension change induced by a vehicle crossing from the south to north direction: (a) before; and (b) after conducting the peak match

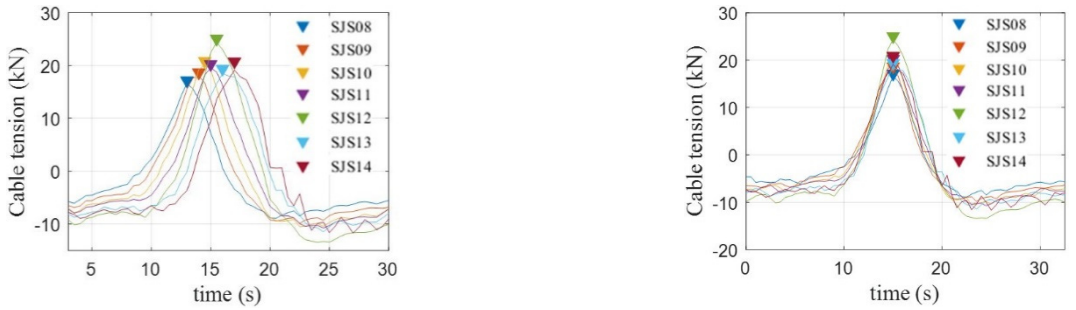

(a) (b)

Fig. 11 The cable tension change induced by a vehicle crossing from the north to south direction: (a) before; and (b) after conducting peak match

between a cable pair, which will be used as a damage feature and further illustrated in Section 4 of this study. A schematic diagram is presented in Fig. 9 for better understanding the process of estimation of the matched cable tension ratio. p and q are defined to represent two cables located on the same side of the bridge. In Fig. 9, $T_c(p)$ and $T_c(q)$ represent the tension forces of the p-th and q-th cables without vehicles on the bridge, which should be constants. η_p^t and η_q^t denote the transverse cable tension influence coefficients, respectively. $max(\eta_p^l)$ and $max\,(\eta_q^l)$ represent the maximum values of longitudinal cable tension influence coefficients of the p-th and q-th cables, which are bridge condition related constants. $max(T_v(p))$ and $max(T_v(q))$ represent the peak values of tension force of cables p and q, respectively. ΔT_v represents the difference between the peak value and valley value. P denotes the vehicle load applied on the bridge. The matched cable tension ratio can be expressed as

$$\varsigma(p,q) = \frac{\Delta T_v(p)}{\Delta T_v(q)} = \frac{max(T_v(p)) - T_c(p)}{max(T_v(q)) - T_c(q)} \tag{4}$$

As mentioned before, the transverse position of vehicles on bridge is the same for any two cables p and q located on the same riverside. Therefore, the transverse cable tension influence coefficients η_p^t and η_q^t in Fig. 9 are constants. $max(T_v(p))$ and $max(T_v(q))$ denote the peak values of tension forces of the p-th and q-th cables, which can be obtained from the peak matching procedure. Eq. (4) can be transformed as

$$\begin{aligned} &max(T_v(p)) \\ &= \varsigma(p,q)max(T_v(q)) + T_c(p) - \varsigma(p,q)T_c(q) \end{aligned} \tag{5}$$

where $max(T_v(q))$ and $max(T_v(p))$ can be viewed as independent variable and dependent variable. The other terms in Eq. (5) are constants. The scatter plot of peak values of tension forces of the p-th and q-th cables can be obtained when certain amount of peak values subjected to different vehicle load P are available via the peak matching procedure. The matched cable tension ratio $\varsigma(p,q)$ can be estimated from the slope of the scatter plot. By this manner, the valley value corresponding to the cable force without vehicles is not required to estimate $\varsigma(p,q)$. In the next section, the scatter plot of cables SJS08 and SJS09 in day 1 is used to further illustrate how to obtain the matched cable tension ratio.

It should be noted that the peak matching procedure is conducted for each peak. Therefore, moving the cable force to eliminate the time lag effect corresponding to the current peak will not affect matching the next peak. No special treatment is applied to other parts of the data. Only the peak values corresponding to different vehicle loads instead of the sampling points near the peak values are used to obtain the proposed damage feature. Therefore, it is unnecessary to cut the data with a moving window.

4. Case study

The peak values of the processed vehicle induced cable tension force datasets are detected by using the matlab in-built function “findpeaks”. Two crucial parameters, namely the minimum distance of any two adjacent peaks and the minimum height of peak, should be carefully selected. Generally speaking, the smaller these two parameters selected, the more peak values will be detected from the datasets. However, the percentage of false peaks caused by measurement noise will increase when these two parameters are too small. After parameters tuning process, the minimum distance of any two adjacent peak values and the minimum amplitude of peak are set as 5 sampling points and 2 kN, respectively. It means that only one peak will be detected if the time span between two peak values is less than 5 sampling points. Moreover, the vehicle induced cable tension change less than 2 kN is not included in this study. Then, the peak value matching algorithm is employed to eliminate the time lag effect in different cables subjected to the same vehicle load. Scatter plot of the matched cable tension forces between cables SJS08 and SJS09 in day 1 is shown in Fig. 12. This scatter plot shows a strongly positive and linear correlation between the cable tension forces of SJS08 and SJS09. Very few outliers are observed in the datasets.

In Eq. (3), the peak value and valley value of each peak should be acquired to calculate the matched cable tension ratio. However, the valley values are relatively small and usually mixed up with the measurement error. In this paper, the slope of the least squares fitted line of the matched cable tension ratio between two cables is defined as the damage sensitive feature. For this damage indicator, more accurate cable tension ratio can be calculated with the peak values. In this study, the slope is represented by degree.

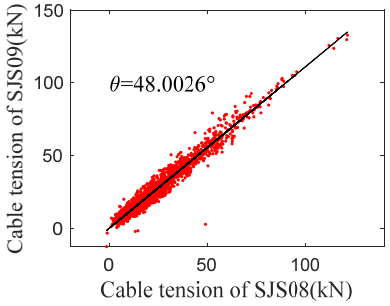

Fig. 12 The matched cable tension ratio between cables SJS08 and SJS09 in day 1

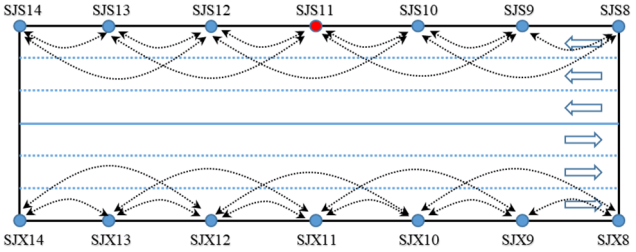

Fig. 13 The designed sensor grouping scheme

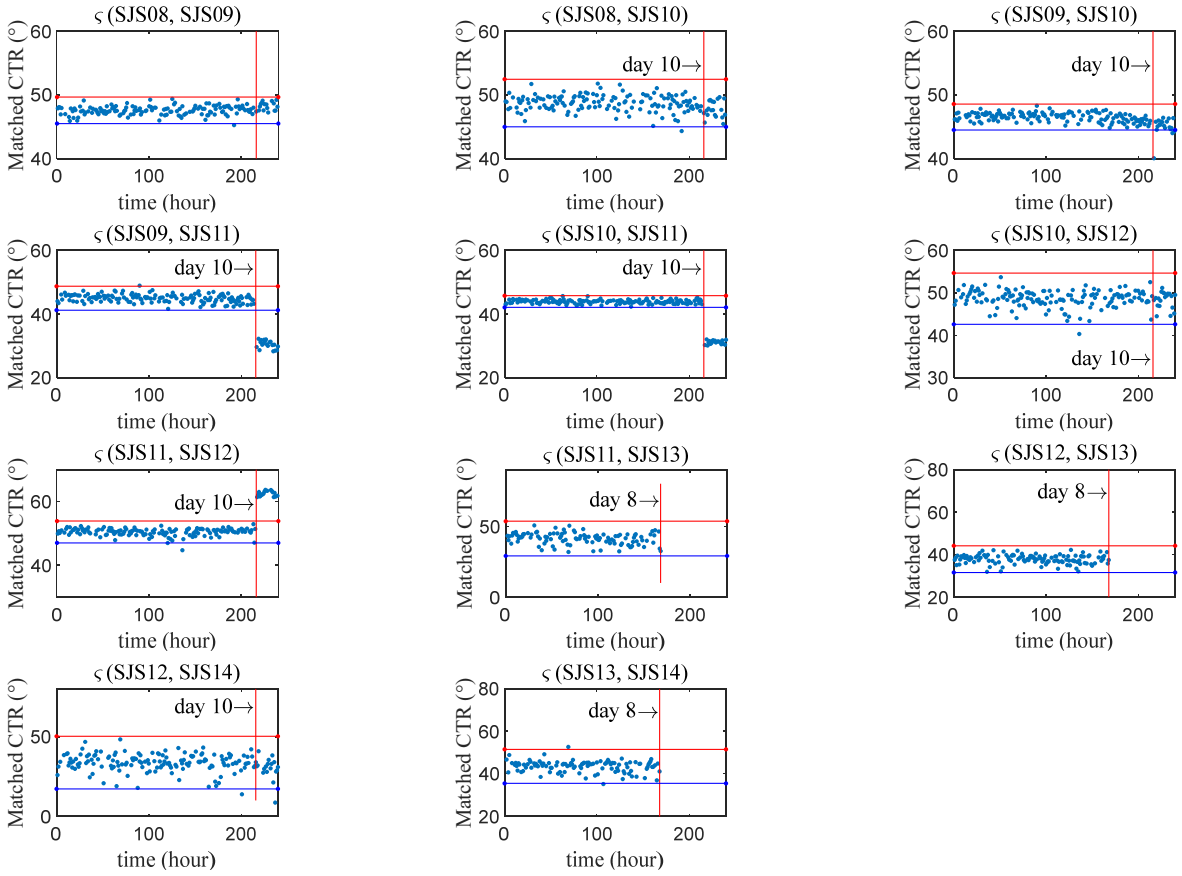

Fig. 14 Evolution results of matched cable tension ratios of cable pairs located on the upstream side. The blue and red lines represent the lower and upper boundaries, respectively.

In fact, any two of the cables located on the same side of the bridge can be paired to calculate the matched cable tension ratio. However, for long span bridges, the overall number of cable pairs is exponentially increased with the number of cables being monitored. With the consideration of computational efficiency, sensors are grouped as according to the following scheme in Fig. 13 to conduct the condition assessment of monitored stay cables. Each cable is paired with the closest two cables located on the same side to ensure that reliable damage identification results can be obtained even when sensor fault occurs in the neighbor of the damaged cable. There are 11 cable pairs on each side of the bridge.

Finally, the hourly matched cable tension ratio of each pair is calculated and results of cable pairs located on the upstream side and downstream side are presented in Fig. 14 and Fig. 15, respectively. To distinguish whether a cable is damaged or not, the control chart is introduced to determine the upper and lower boundaries of the matched cable tension ratio values under the healthy state. Matched cable tension ratio values exceeding or less than the mean value plus 3 times of standard deviation are determined as damaged. The calculations are performed on a desktop with an Intel(R) Core(TM) i7-7700 CPU (3.6 GHz) and 16 GB RAM. The overall computational time of using the proposed approach to process the data of these 14 cables within 10 days and an hour are 51.22 s and 0.21 s, respectively, which is time efficient for online SHM application.

As observed from Figs. 14 and 15, the damage indicator based on the matched cable tension ratio defined in this study is stable with less oscillations, which means that the proposed approach is robust to environmental effects, measurement noise and different vehicle patterns as shown in Fig. 8. It should be noted that the damage indicator, namely, matched cable tension ratio, is abbreviated as matched CTR as shown in Figs. 14 and 15. Abrupt change in the matched cable tension ratios is found in cable pairs SJS09-SJS11, SJS10-SJS11 and SJS11-SJS12 in day 10 (marked by the red dotted line in Fig. 14). The damage index values (matched cable tension ratios) of those three cable pairs in day 10 exceed the upper or lower boundaries, which indicates that damage occurs in one of these three cables. Since these three cable pairs are all related to cable SJS 11, therefore, it can be confidently concluded that the damage has occurred in this cable. It should be noted that the sensor fault occurred in cable SJS13 from day 8 to day 10, as described in Section 2.1. Therefore, cable pair SJS11-SJS13 has no results since day 8 owning to the sensor fault, and is unable to detect the damage of SJS11. The results from any sensor pair of the downstream side are consistent through the datasets obtained in these 10 days. No abrupt change is observed in any sensor pair, as shown in Fig. 15, indicating that no cable damage occurs on the downstream side. These damage detection results demonstrate that the proposed approach is reliable and efficient to detect the

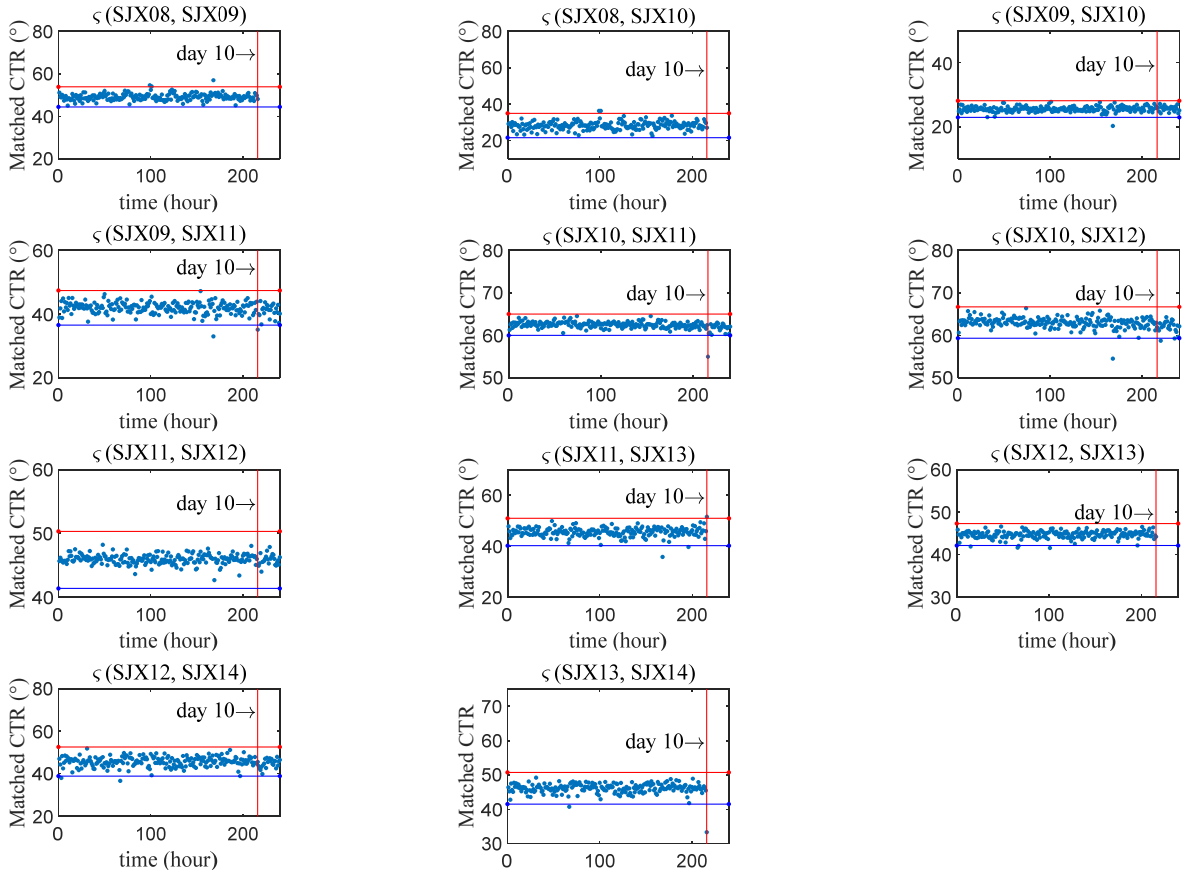

Fig. 15 Evolution results of matched cable tension ratios of cable pairs located on the downstream side. The blue and red lines represent the lower and upper boundary, respectively.

damage in cables of this cable-stayed bridge, with the awareness of sensor fault and the consideration of operational conditions with different traffic patterns.

The performance of the proposed approach for damage detection in stay cables is quantified with the well-known metrics, with the accuracy, precision, recall and F1 score being defined as follows

$$\text{Accuracy} = \frac{TP + TN}{TP + TN + FP + FN} \times 100\% \tag{6}$$

$$\text{Precision} = \frac{TP}{TP + FP} \times 100\% \tag{7}$$

$$\text{Recall} = \frac{TP}{TP + FN} \times 100\% \tag{8}$$

$$\text{F1 score} = 2 * \frac{Precision * Recall}{Precision + Recall} \times 100\% \tag{9}$$

in which, True Negative (*TN*) means that the ground truth is false and the detection result is also false; False Positive (*FP*) means that the ground truth is false while the detection result is true; False Negative (*FN*) means that the ground truth is true while the detection result is false; and True Positive (*TP*) means that the ground truth is true and the detection result is also true.

According to the results presented in Figs. 14 and 15, damage has occurred in cable SJS11. The damage identification results of all the cable pairs in Figs. 14 and 15 are used to quantify the performance of the proposed cable damage detection method. Table 1 shows the performance metrics of the proposed approach for cable damage detection. All the four performance metrics are above 95%. In particular, the 100% recall value indicates that the proposed matched cable tension ratio damage index is able to alarm the damage occurred in cable SJS11 at the last day with no false identification. Only very few false positive alarms occur in the first 9 days, the accuracy and precision are slightly affected. Overall, the proposed matched cable tension ratio damage index is reliable to identify and locate the damaged cable.

Table 1 Performance metrics of the proposed cable damage detection method

Accuracy	Precision	Recall	F1 score
97.97%	95.08%	100%	97.48%

5. Conclusions

In this study, a novel and physically interpretable damage detection approach for cables in cable-stayed bridges is proposed. To eliminate the influence of vehicle

transverse position on the cable tension ratio between any two cables located on the same side, a peak matching procedure is used to process the vehicle induced cable tension forces. A sensor grouping scheme is designed to ensure the computational efficiency with the awareness of sensor fault. Matched cable tension ratios are obtained for damage detection in stay cables under different traffic patterns. Slope of the curve-fitted linear relationship in matched cable tension ratios between two cables is used as damage sensitive feature. An in-service cable-stayed bridge installed with long-term stay cable force monitoring system is used to validate the effectiveness and accuracy of using the proposed approach for condition assessment of cables. Identification results indicate that the damage occurred in the stay cable can be accurately detected under the operational conditions irrespective of traffic patterns and considering the sensor fault. The proposed approach also overcomes the limitation of existing methods by using the cable pair from two cables on the opposite sides of the cable-stayed bridges to detect the damage in cables, and using the monitoring data separated from scenarios with specific vehicle loading pattern. The proposed approach is robust to the traffic patterns, locations of paired cables, operational conditions and even sensor fault.

Acknowledgments

The authors would like to thank the organizations of the International Project Competition for SHM (IPC-SHM 2020) ANCRiSST, Harbin Institute of Technology (China), and University of Illinois at Urbana-Champaign (USA) for their generously providing the invaluable data from actual structures. The authors also would like to thank the chairs of IPC-SHM 2020 Prof. Hui Li, and Prof. Billie F. Spencer Jr. for their leadership on the competition.

References

Alamdari, M.M., Kildashti, K., Samali, B. and Goudarzi, H.V. (2019), "Damage diagnosis in bridge structures using rotation influence line: Validation on a cable-stayed bridge", *Eng. Struct.*, **185**, 1-14. https://doi.org/10.1016/j.engstruct.2019.01.124

Bao, Y., Li, H., Chen, Z., Zhang, F. and Guo, A. (2016), "Sparse l1 optimization-based identification approach for the distribution of moving heavy vehicle loads on cable-stayed bridges", *Struct. Control Health Monitor.*, **23**(1), 144-155. https://doi.org/10.1002/stc.1763

Bao, Y., Li, J., Nagayama, T., Xu, Y., Spencer Jr, B.F. and Li, H. (2021), "The 1st International Project Competition for Structural Health Monitoring (IPC-SHM, 2020): A summary and benchmark problem", *Struct. Health Monitor.*, 14759217211006485. https://doi.org/10.1177/14759217211006485

Chen, Z.W., Zhu, S., Xu, Y.L., Li, Q. and Cai, Q.L. (2015), "Damage detection in long suspension bridges using stress influence lines", *J. Bridge Eng.*, **20**(3), 05014013. https://doi.org/10.1061/(ASCE)BE.1943-5592.0000681

Chen, C.C., Wu, W.H., Liu, C.Y. and Lai, G. (2016), "Damage detection of a cable-stayed bridge based on the variation of stay cable forces eliminating environmental temperature effects", *Smart Struct. Syst., Int. J.*, **17**(6), 859-880. https://doi.org/10.12989/sss.2016.17.6.859

Davalos, E. (2000), "Structural behaviour of cable-stayed bridges", Ph.D. Dissertation; Massachusetts Institute of Technology.

Fan, G., Li, J. and Hao, H. (2019), "Lost data recovery for structural health monitoring based on convolutional neural networks", *Struct. Control Health Monitor.*, **26**(10), e2433. https://doi.org/10.1002/stc.2433

Fan, Z.Y., Huang, Q., Ren, Y., Zhu, Z.Y. and Xu, X. (2020a), "A cointegration approach for cable anomaly warning based on structural health monitoring data: An application to cable-stayed bridges", *Int. J. Adv. Struct. Eng.*, **23**(13), 2789-2802. https://doi.org/10.1177/1369433220924793

Fan, G., Li, J. and Hao, H. (2020b), "Vibration signal denoising for structural health monitoring by residual convolutional neural networks", *Measurement*, **157**, 107651. https://doi.org/10.1016/j.measurement.2020.107651

Feng, D., Scarangello, T., Feng, M.Q. and Ye, Q. (2017), "Cable tension force estimate using novel noncontact vision-based sensor", *Measurement*, **99**, 44-52. https://doi.org/10.1016/j.measurement.2016.12.020

Guo, W.H. and Xu, Y.L. (2001), "Fully computerized approach to study cable-stayed bridge–vehicle interaction", *J. Sound Vib.*, **248**(4), 745-761. https://doi.org/10.1006/jsvi.2001.3828

Kangas, S., Helmicki, A., Hunt, V., Sexton, R. and Swanson, J. (2012), "Cable-stayed bridges: case study for ambient vibration-based cable tension estimation", *J. Bridge Eng.*, **17**(6), 839-846. https://doi.org/10.1061/(ASCE)BE.1943-5592.0000364

Kim, S.W., Jeon, B.G., Cheung, J.H., Kim, S.D. and Park, J.B. (2017), "Stay cable tension estimation using a vision-based monitoring system under various weather conditions", *J. Civil Struct. Health Monitor.*, **7**(3), 343-357. https://doi.org/10.1007/s13349-017-0226-7

Kullaa, J. (2013), "Detection, identification, and quantification of sensor fault in a sensor network", *Mech. Syst. Signal Process*, **40**(1), 208-221. https://doi.org/10.1016/j.ymssp.2013.05.007

Li, H. and Ou, J.P. (2016), "The state of the art in structural health monitoring of cable-stayed bridges", *J. Civil Struct. Health Monitor.*, **6**(1), 43-67. https://doi.org/10.1007/s13349-015-0115-x

Li, H., Li, S., Ou, J. and Li, H. (2012), "Reliability assessment of cable-stayed bridges based on structural health monitoring techniques", *Struct. Infrastruct. Eng.*, **8**(9), 829-845. https://doi.org/10.1080/15732479.2010.496856

Li, J., Hao, H. and Zhu, H.P. (2014), "Dynamic assessment of shear connectors in composite bridges with ambient vibration measurements", *Adv. Struct. Eng.*, **17**(5), 617-637. https://doi.org/10.1260/1369-4332.17.5.617

Li, S., Wei, S., Bao, Y. and Li, H. (2018), "Condition assessment of cables by pattern recognition of vehicle-induced cable tension ratio", *Eng. Struct.*, **155**, 1-15. https://doi.org/10.1016/j.engstruct.2017.09.063

Liu, C., Teng, J. and Peng, Z. (2020), "Optimal sensor placement for bridge damage detection using deflection influence line". *Smart Struct. Syst., Int. J.*, **25**(2), 169-181. https://doi.org/10.12989/sss.2020.25.2.169

Martins, A.M., Simões, L.M. and Negrão, J.H. (2015), "Cable stretching force optimization of concrete cable-stayed bridges including construction stages and time-dependent effects", *Struct. Multidiscip. Optim.*, **51**(3), 757-772. https://doi.org/10.1007/s00158-014-1153-4

Nghia, N.T. and Samec, V. (2016), "Cable stay bridges investigation of cable rupture". *Int. J. Civil Eng. Archit.*, **10**, 270-279. https://doi.org/10.17265/1934-7359/2016.05.006.

Stromquist-LeVoir, G., McMullen, K.F., Zaghi, A.E. and Christenson, R. (2018), "Determining time variation of cable

tension forces in suspended bridges using time-frequency analysis", *Adv. Civil Eng*., 2018. https://doi.org/10.1155/2018/1053232

Vivó-Truyols, G., Torres-Lapasio, J.R., Van Nederkassel, A.M., Vander Heyden, Y. and Massart, D.L. (2005), "Automatic program for peak detection and deconvolution of multi-overlapped chromatographic signals: Part I: Peak detection", *J. Chromatogr. A*, **1096**(1-2), 133-145. https://doi.org/10.1016/j.chroma.2005.03.092

Xu, Z.D. and Wu, Z. (2007), "Simulation of the effect of temperature variation on damage detection in a long-span cable-stayed bridge", *Struct. Health Monitor*, **6**(3), 177-189. https://doi.org/10.1177/1475921707081107

Zhang, L.X., Qiu, G.Y. and Chen, Z.S. (2020), "Structural health monitoring methods of cables in cable-stayed bridge: A review", *Measurement*, 108343. https://doi.org/10.1016/j.measurement.2020.108343